ARTICLE

doi:10.1016/j.ymthe.2005.06.002

Prolonged Recovery of Retinal Structure/Function after Gene Therapy in an *Rs1h*-Deficient Mouse Model of X-Linked Juvenile Retinoschisis

Seok H. Min,[1,*] Laurie L. Molday,[2] Mathias W. Seeliger,[3] Astra Dinculescu,[1] Adrian M. Timmers,[1] Andreas Janssen,[4] Felix Tonagel,[3] Naoyuki Tanimoto,[3] Bernhard H. F. Weber,[4] Robert S. Molday,[2] and William W. Hauswirth[1,5]

[1]*Department of Ophthalmology and* [5]*Department of Molecular Genetics and Microbiology and Gene Therapy Center, University of Florida College of Medicine, Gainesville, FL 32610, USA*

[2]*Department of Biochemistry and Molecular Biology and Department of Ophthalmology, Centre for Macular Research, University of British Columbia, Vancouver, BC, Canada V6T 1Z3*

[3]*Retinal Electrodiagnostics Research Group, Department of Pathophysiology of Vision and Neuroophthalmology, University of Tübingen, D-72076 Tübingen, Germany*

[4]*Institute of Human Genetics, University of Regensburg, D-93053 Regensburg, Germany*

**To whom correspondence and reprint requests should be addressed at the Department of Ophthalmology, Box 100284, University of Florida, Gainesville, FL 32610, USA. Fax: (352) 392 3062. E-mail: smin@eye.ufl.edu.*

Available online 18 July 2005

X-linked juvenile retinoschisis (RS) is a common cause of juvenile macular degeneration in males. RS is characterized by cystic spoke-wheel-like maculopathy, peripheral schisis, and a negative (b-wave more reduced than a-wave) electroretinogram (ERG). These symptoms are due to mutations in the *RS1* gene in Xp22.2 leading to loss of functional protein. No medical treatment is currently available. We show here that in an *Rs1h*-deficient mouse model of human RS, delivery of the human *RS1* cDNA with an AAV vector restored expression of retinoschisin to both photoreceptors and the inner retina essentially identical to that seen in wild-type mice. More importantly, unlike an earlier study with a different AAV vector and promoter, this work shows for the first time that therapeutic gene delivery using a highly specific AAV5–opsin promoter vector leads to progressive and significant improvement in both retinal function (ERG) and morphology, with preservation of photoreceptor cells that, without treatment, progressively degenerate.

Key Words: retinoschisis, knockout mouse, gene therapy, AAV vector, electroretinogram, opsin promoter

INTRODUCTION

X-linked juvenile retinoschisis (RS) is a recessive degenerative disease of the central retina affecting only males with a worldwide prevalence estimated at 1/5000–1/25,000 [1]. The disease may develop as early as infancy, but is more often detected in boys between 5 and 10 years of age due to reading difficulties in school. Affected individuals have a relatively normal a-wave in the electroretinogram (ERG), while the b-wave is nearly or totally absent. Another hallmark of RS is the star-shaped schisis or splitting of the inner retina, which develops primarily in the fovea, but can also be present in the peripheral retina. These cystoid cavities may coalesce, leading to further visual acuity loss. Later in life, total vision loss can occur as a result of associated complications such as retinal detachment, vitreal hemorrhage, or choroidal sclerosis.

The gene responsible for retinoschisis was identified by positional cloning within chromosome band Xp22.2 [2]. It consists of six exons and encodes a 224-amino-acid protein that includes a 23-residue secretory leader sequence. The encoded protein, termed RS1 or retinoschisin, is secreted from both photoreceptors and bipolar cells as a multimeric complex consisting of identical subunits linked together by disulfide bonds [3–5]. Each subunit consists of a single discoidin domain that has been implicated in cellular adhesion and cell–cell interactions. Currently, 133 different disease-causing mutations are known, of which 111 are located within the discoidin domain (http://www.dmd.nl/rs/). The effect of a number of these mutations has been examined at a molecular and cellular level [5,6]. Missense mutations in the discoidin domain cause protein misfolding and retention of RS1 in

1525-0016/$30.00

the endoplasmic reticulum (ER), while mutations in the leader sequence prevent the translocation of the polypeptide chain across the ER membrane as part of the secretion process. Mutations in cysteine residues flanking the discoidin domain cause defective disulfide-linked subunit assembly. In each case the mutant protein is unable to function as an extracellular cell adhesion protein. Since female carriers are unaffected, the absence of a functional RS1 protein rather than the presence of a mutant protein is responsible for RS in affected males.

To gain insight into the functional aspects of retinoschisin, we generated a knockout (KO) mouse deficient in *Rs1h* [7], the murine ortholog of the human retinoschisis gene, *RS1* [8]. The *Rs1h*-deficient mouse shares several important diagnostic features with human RS, including the typical negative ERG response, development of cystic structures within the inner retina, and the loss of photoreceptor cells [7,9]. Thus, the *Rs1h* KO mouse is a valuable model for developing potential therapeutic interventions for human RS. To explore this goal, we generated a construct containing the human *RS1* cDNA under the control of the mouse opsin promoter in a recombinant adeno-associated virus (AAV) serotype 5 vector and tested it for therapeutic efficacy in *Rs1h*-deficient mice. We show here that delivery of the human *RS1* cDNA to *Rs1h*-deficient mice using an AAV5–opsin promoter vector restored the expression of retinoschisin to both photoreceptors and the inner retina essentially identical to that seen in wild-type mice. Moreover, unlike a previous study in which a different AAV vector and promoter was used [10], we provide evidence that the therapeutic gene expression leads to both progressive and significant improvement in retinal function (ERG) and morphology with preservation of photoreceptor cells.

RESULTS

Vector-Mediated Expression of RS1 Leads to Improved *in Vivo* Retinal Topography in the *Rs1h*-Deficient Mouse

We delivered a capsid serotype 5 AAV vector containing the wild-type human *RS1* cDNA driven by a mouse opsin promoter (AAV5-mOP-RS1) into the subretinal space of the right eyes of *Rs1h*-deficient 15-day-old mice. Contralateral left eyes were not injected and served as internal controls. To confirm that AAV5-mOP-RS1 led to expression of the retinoschisin protein, we labeled a Western blot of total protein from three pooled treated and untreated retinas with a monoclonal antibody directed against human RS1 [7]. The 24-kDa RS1-specific protein band was present in the retinal extracts from the AAV5-mOP-RS1-injected eyes, but absent in the contralateral controls, indicating that retinoschisin expression occurs upon treatment (Fig. 1).

In vivo analysis of retinal morphology with scanning-laser ophthalmoscopy (SLO) revealed a prominent structural difference between treated and untreated eyes 6 months after injection (Fig. 2). The pathological pattern of evenly distributed mottling originates from cyst formation in the inner retina [7] and is clearly evident in uninjected eyes (Fig. 2, right), whereas in treated eyes the appearance of the inner retina is unremarkable in regions where the vector was delivered, very similar to wild type (Fig. 2, left and middle). A minor pigmentation change surrounds the site of injection, indicative of a small retinal detachment following injection (Fig. 2, arrowheads).

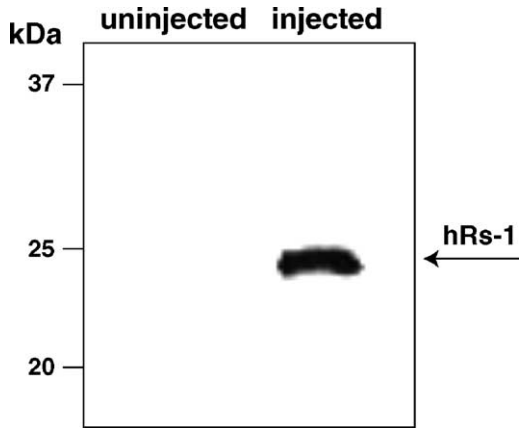

FIG. 1. RS1 expression in retinas of AAV-mOP-hRS1-injected and uninjected eyes. Retinal homogenates from treated and untreated eyes were separated on a 10% SDS–polyacrylamide gel and the Western blot was probed with the RS1 3R10 monoclonal antibody. A single 24-kDa band corresponding to RS1 was detected in the AAV-mOP-hRS1-injected retinas, but not in the uninjected contralateral controls. The positions of prestained molecular mass markers (in kDa) are indicated on the left.

Vector-Mediated Expression of RS1 Restores both Rod- and Cone-Mediated ERG Responses in the *Rs1h*-Deficient Mouse

To gain a preliminary impression of the functional consequences of RS1 replacement, we followed the maximum rod-mediated (scotopic) ERG amplitudes at regular intervals for 3 months (Fig. 3). ERG b-wave amplitudes in untreated eyes decline with time, confirming previous observations [7]. In contrast, delivery of AAV5-mOP-RS1 vector reversed this trend and was able to improve b-wave amplitudes at 2 and 3 months posttreatment relative to 1 month. A similar trend was also apparent for the rod-mediated a-wave with stable a-wave amplitudes in treated retinas over the 3-month period.

We then carried out a more detailed electroretinographic analysis on a separate cohort of animals treated in one eye 5 months previously. Scotopic single-flash ERG indicated a significant recovery of the negative ERG waveform in treated versus untreated eyes (Figs. 4a and 4c). An increased b-wave was apparent at higher stimulus intensities, with a modest increase in rod-mediated

doi:10.1016/j.ymthe.2005.06.002

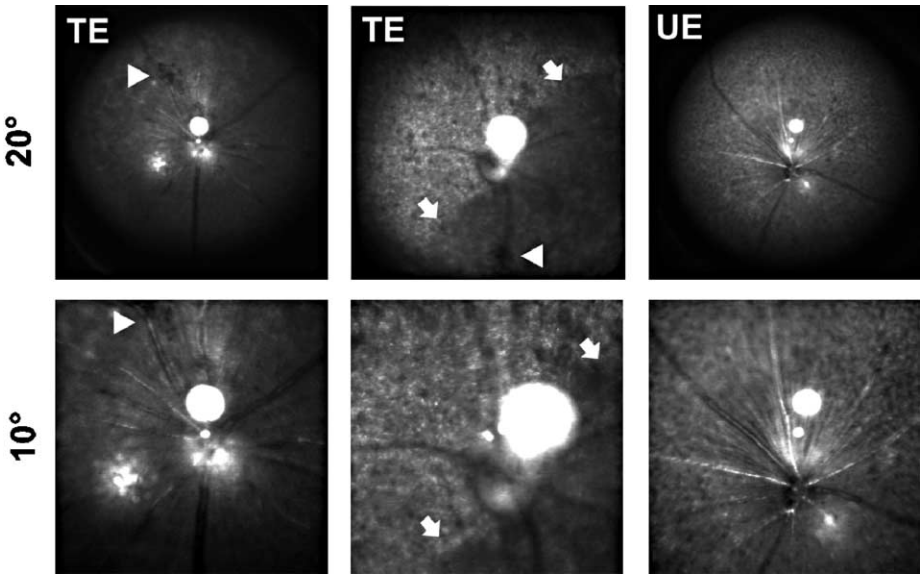

FIG. 2. *In vivo* imaging of AAV-mOPs-hRS1-injected and uninjected eyes. 10° and 20° indicate the magnification of the fundus photographs reflecting the instrument setting. Red-free (514.5 nm) laser images demonstrate the typical pattern of Rs1h-deficient lesions in the uninjected eye (UE) and the dramatic improvement in the treated eyes (TE). The site of injection (arrowhead) and the discoloration caused by the postinjection changes are visible. The extent of the treated area varied from almost complete (left column) to about 40% (center column). In the latter case, the border of the treated area is marked with arrows.

amplitudes in nearly all animals studied (Fig. 4e, left). An even more pronounced effect of treatment was observed in the light-adapted (photopic) single-flash ERG (Figs. 4b and 4c) arising mainly from the recovery of oscillatory potentials (OPs). The most prominent difference was seen in the photopic flicker ERG (Figs. 4d and 4e). In addition to improved OPs, responses to stimulus frequencies above 3–5 Hz were greatly improved in treated eyes.

Vector-Mediated Expression of RS1 Restores Normal Retinal Distribution of RS1 Protein in the *Rs1h*-Deficient Mouse and Corrects a Variety of Retinal Structural Defects

To determine the treatment effect on the tissue distribution of retinoschisin, we used a monoclonal antibody to RS1 to label cryosections of retinas from 5-month posttreatment retinas, untreated *Rs1h*-deficient mouse retinas, and retinas of age-matched C57BL/6 wild-type mice. Patterns of RS1 labeling in injected retinas were remarkably similar to those of wild-type mice (Figs. 5a–5c). Photoreceptor inner segments showed intense RS1 staining while outer nuclear and outer plexiform layers were also labeled. There was additional distinct immunostaining in the inner nuclear (bipolar) layer and inner plexiform layer. Typically, only the peripheral regions of the retina, distant from the site of injection, exhibited a relative absence of RS1 labeling. Improvements in retinal structure were highlighted by differential interference contrast images stained with DAPI nuclear dye (Figs. 5d–5f). Untreated eyes showed pronounced disorganization at the zone between inner and outer nuclear layers where numerous gaps of various sizes within the bipolar cell layer were evident. In contrast, treated eyes showed a distinct separation of inner and outer nuclear layers similar to that observed in wild-type retinas, an absence of gaps between bipolar cells, and an increase in the thickness of the outer nuclear layer. The outer nuclear layer of the injected eye had an average of 10.5 ± 1.0 photoreceptor nuclei per column of cell bodies, whereas the untreated contralateral retina had only 7.7 ± 1.5 nuclei. Treated retinas showed a narrow, well-defined band of synaptophysin labeling of the photoreceptor–bipolar synaptic region, whereas the untreated retina displayed a much more irregular labeling pattern (Figs. 5g–5i). Likewise, bipolar cells in treated retinas exhibited an organized arrangement of cells akin to that of a wild-type retina, whereas the untreated retinas displayed bipolar cell disorganization (Figs. 5j–5l). GFAP, normally expressed at low levels in the basal region of retinal Müller cells [11], was markedly upregulated in the untreated retina (Fig. 5o), consistent with observations associated with a variety of retinal lesions [12,13]. Treated *Rs1h*-deficient retinas exhibited nearly normal GFAP expression levels (Figs. 5m–5o). Additionally, the thickness of the outer nuclear layer was greater in the retinas of the treated eye compared to the untreated eye (8.5 ± 1.2 vs 6.9 ± 0.8, $n = 5$). Preliminary studies indicate that these structural improvements last more than 1 year.

DISCUSSION

AAV-vectored RS1 restored both retinal integrity and function in an *Rs1h*-deficient mouse model of human RS. AAV-RS1 treatment not only partially corrected the negative ERG, one of the hallmarks of both the RS

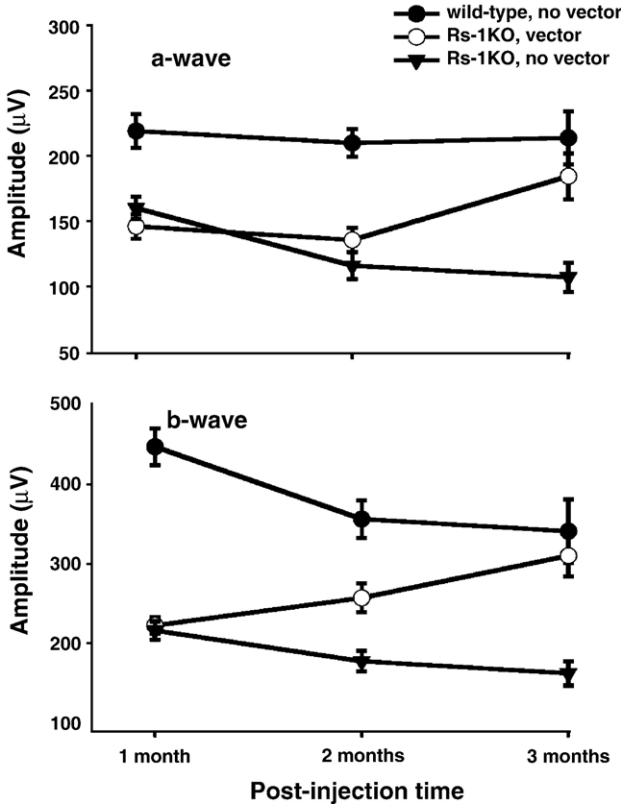

FIG. 3. Preliminary electrophysiological response of AAV-mOP-RS1-injected and uninjected eyes from *RS1h*-deficient mice. Simultaneous bilateral full-field scotopic maximum ERG amplitudes in eyes of *Rs1h*-deficient mice at 1, 2, and 3 months postinjection. Bars represent mean amplitudes ± SEM of 15, 15, and 15 eyes at 1, 2, and 3 months postinjection, respectively. Normal ERG amplitudes of wild-type mice at comparable ages are shown for comparison. *P* value between ''KO, no vector'' and ''KO, vector'' groups was obtained with Student's paired *t* test. Values are the averages of five responses to a stimulus intensity of 0.173 log cd s m^{-2} with a 1-min dark interval between each recording. The values of a-wave amplitudes between injected and uninjected eyes at 3 months postinjection are statistically significant (184.9 ± 17.5 μV vs 107.4 ± 11.2 μV, $P < 0.001$). The values of b-wave amplitudes between treated and untreated eyes are 257.7 ± 18.2 μV vs 177.9 ± 13.0 μV ($P < 0.001$) at 2 months postinjection and 310.9 ± 25.8 μV vs 162.6 ± 15.3 μV ($P < 0.001$) at 3 months postinjection, respectively.

patient and the *Rs1h*-deficient mouse, but resulted in improved visual function over approximately half the lifetime of a mouse. The scotopic single-flash ERG showed clear b-wave improvement, and even more prominent photopic single-flash ERG recovery, with the largest benefit seen in the flicker responses and OPs. Since these ERG elements are each believed to derive largely from postphotoreceptor responses, the major therapeutic effect is suggested to involve functional improvement in the inner retina. This correlates well with both the histological findings and the results of *in vivo* imaging demonstrating the structural improvements and near elimination of inner retinal schisis achieved by this treatment.

Onset of AAV5-RS1 expression in photoreceptors is known to be fast, as early as 2 weeks after injection. It is unclear at this stage why a peak of both a- and b-waves is reached only 3 months after injection. We are currently investigating the possibility that delivery of the therapeutic gene may be able to repair early stage retinoschisis and this process may take time, thus explaining the delay in reaching the maximum ERG response following treatment.

The broadly distributive pattern of RS1 expression in treated eyes is nearly identical to that seen in wild-type mice. It suggests that retinoschisin, expressed either naturally in wild-type mice or via an AAV vector in the KO photoreceptors, is capable of moving longitudinally and possibly also laterally within the retina to its normal extracellular target sites. This observation contrasts with the preliminary work of Zeng *et al.* [10], who employed a similar approach but used a different mouse model and vector. They report high levels of RS1 expression not only in photoreceptors but also in ganglion cells after AAV2-cytomegalovirus (CMV)-RS1 treatment. This difference likely reflects different experimental conditions, principally the AAV vector serotype and promoter. Although serotype 2 and 5 vectors transduce both photoreceptors and retinal pigmented epithelium, the latter is much more efficient at transducing photoreceptors in the mouse retina than the former when delivered into the subretinal space [14,15]. Furthermore, the specificity of AAV-mediated mouse photoreceptor transduction is improved by replacing the CMV promoter with the rod opsin promoter as was done in our study [16]. In addition, it is well documented that serotype 2 AAV vectors transduce retinal ganglion cells (RGC) upon intravitreal but not upon subretinal injection [17,18]. Therefore, it is possible that the RGC transduction noted by Zeng *et al.* [10] reflects some leakage of vector into the vitreous space during the subretinal injection. Given the photoreceptor specificity of expression with our AAV5–opsin promoter vector, it is very likely that photoreceptors are the primary source of RS1 for retina. It is also important to note that in our study morphological recovery of the inner retina and photoreceptors accompanies improvement in visual function. This observation contrasts with the previous study [10], in which improvement of retinal function was not accompanied by corresponding changes in retinal morphology. Perhaps the potentially higher levels of RS1 related to our selection of AAV serotype and promoter account for this key difference.

In conclusion, the present study demonstrates that gene therapy can effectively restore visual function in an *Rs1h*-deficient mouse for at least 5 months postinjection. This visual improvement is linked to the recovery of

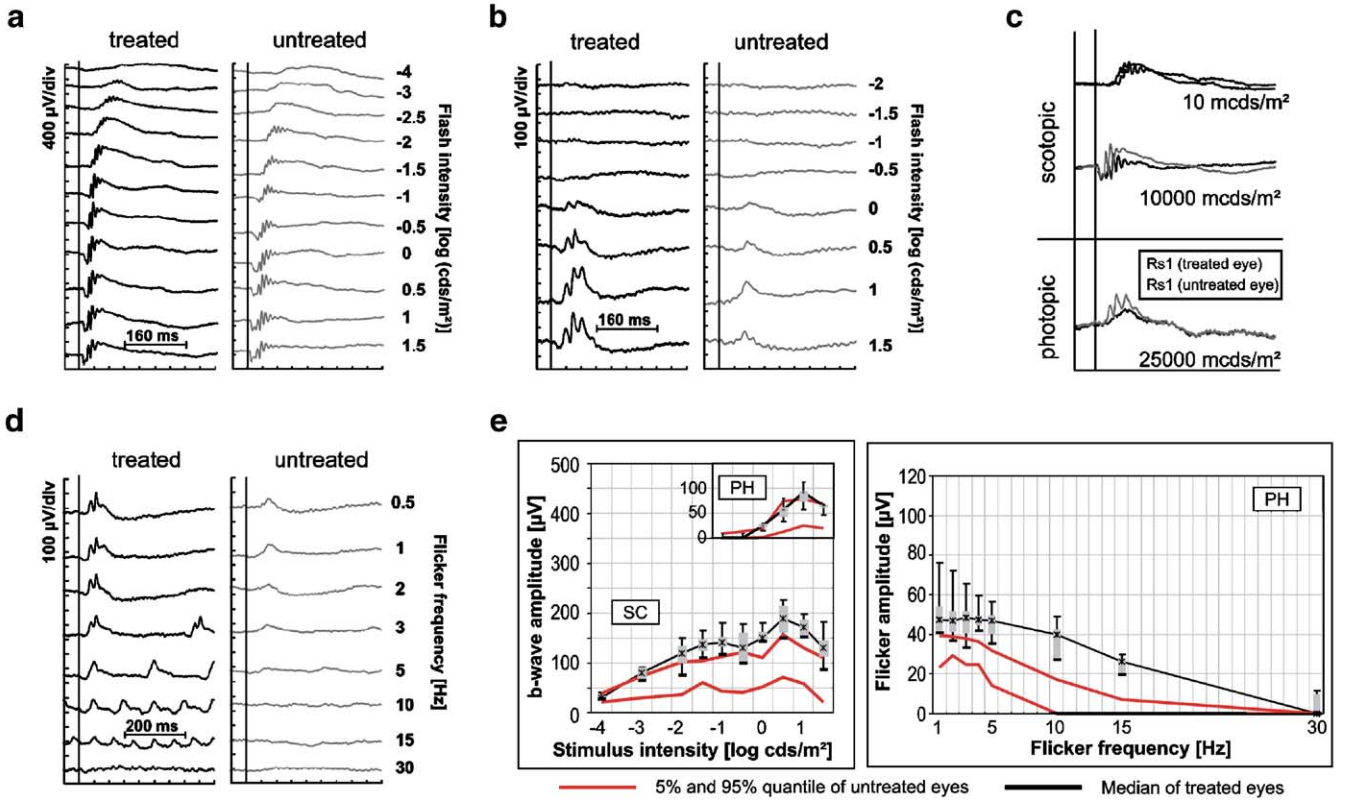

FIG. 4. Electrophysiological evaluation of AAV-mOP-hRS1-injected and uninjected eyes from *RS1h*-deficient mice at 5 months posttreatment. (a) Scotopic (dark-adapted) intensity series of a treated animal. Differences between the treated and the untreated eye are apparent mainly at higher flash intensities, illustrating the recovery from the negative ERG waveform shape. (b) Photopic (light adapted) intensity series of a treated animal. Differences between the treated and the untreated eye are more pronounced due to the strongly reduced or lacking oscillatory potentials in the untreated eye. (c) Overlay of selected scotopic (top) and photopic (bottom) waveforms from the intensity series of a treated animal to illustrate differences in waveform between the treated and the untreated eye. (d) Photopic flicker series of a treated animal. Prominent differences between the treated and the untreated eye are seen, indicating a recovery particularly for frequencies above 3–5 Hz. (e) Dark-adapted (SC) and light-adapted (PH) b-wave and flicker amplitudes from treated eyes as a function of the logarithm of the flash intensity and the flicker frequency, respectively. In both graphs, data from the treated eyes are given as box-and-whisker plots showing 5 and 95% quantiles (whiskers), 25 and 75% quartiles (box), and the median (marked by a cross). The red lines delimit the range given by the 5 and 95% quantile of the untreated eyes.

MOLECULAR THERAPY Vol. 12, No. 4, October 2005

doi:10.1016/j.ymthe.2005.06.002

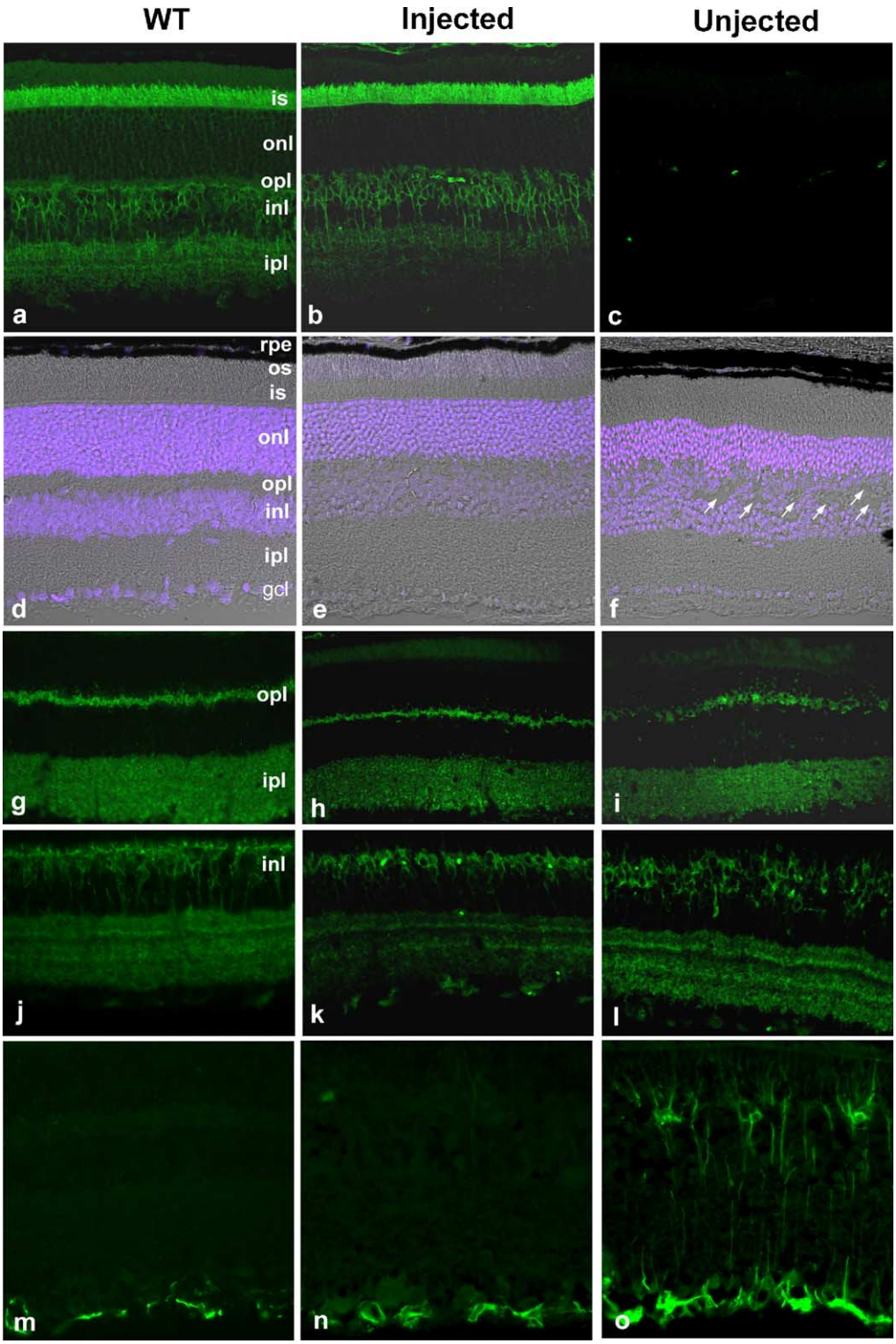

FIG. 5. Immunofluorescence microscopy of retinas from AAV-mOP-hRS1-injected and uninjected *Rs1h*-deficient mice at 5 months posttreatment. Retinal cryosections were (a–c) labeled with the RS1 3R10 monoclonal antibody and (d–f) stained with DAPI nuclear stain (blue) and imaged with differential interference contrast microscopy, (g–i) labeled with SVP38 monoclonal antibody to synaptophysin, (j–l) labeled with the 115A10 monoclonal antibody to bipolar cells and stained with anti-GFAP (m–o) to assess the Müller cell response to retinal lesions. Immunolabeling was visualized using Alexa 488-conjugated goat-anti-mouse Ig. Arrows show gaps present in the untreated *Rs1h*-deficient mice. rpe, retinal pigment epithelium; os, outer segment; is, inner segment; onl, outer nuclear layer; opl, outer plexiform layer; inl, inner nuclear layer; ipl, inner plexiform layer; gcl, ganglion cell layer.

doi:10.1016/j.ymthe.2005.06.002

impaired retinal morphology within both the inner and the outer retinal layers. In preliminary results, such functional and structural recovery persists for a longer period.

MATERIALS AND METHODS

Rs1h-Deficient Animals

The *Rs1h* knockout mouse has been previously described [7]. Since then, the targeted *Rs1h* gene has been bred for 10 generations onto a CB57BL/6 background. Heterozygous *Rs1h* animals were inbred to generate either homozygous *Rs1h* females or hemizygous $Rs1h^{-/Y}$ males. *Rs1h*-ko mice were screened by pcr amplification using tail dna as the template, with two sets of oligonucleotide primers. one set (5′-TGAGGACCCCTGGTACCAGAA-3′, 5′-CCATCTCAGGCAAGCCAGG-3′) was designed to amplify the wild-type *Rsh1* gene, targeting exon 3 with a product size of 260 bp. The same 5′ primer, in combination with a 3′ primer (5′-CAAGGCGATTAAGTTGGGTAAC-3′) targeting LacZ was used to detect the mutant *Rs1h* gene with a product size of 180 bp. A total of 15 *Rs1h*-deficient mice were used in this study. The animals were reared under standard laboratory conditions (22 ± 2°C, 60 ± 10% relative humidity, and a 12-h light–dark cycle) and had free access to food and water throughout the experiment. C57BL/6 wild-type mice used as controls were obtained from The Jackson Laboratory (Bar Harbor, ME, USA). The conditions of housing and experiments were in accordance with the ARVO *Statement for the Use of Animals in Ophthalmic and Vision Research* using protocols approved by the University of Florida Institutional Animal Care and Use Committee.

Construction of an AAV Vector Expressing Human RS1

A cDNA encoding the full-length human RS1 was initially cloned into the vector pBlueScript and then recloned into a pTR-AAV plasmid and includes AAV inverted terminal repeats; a proximal mouse opsin promoter (mOP-500), which restricts expression to photoreceptors; and the human *RS1* cDNA. Titers of AAV serotype 5 vectors were adjusted to 4×10^{13} vector genomes/ml. Ratios of physical to infectious particles were all lower than 100. For the production of the vector, a mini-Ad helper plasmid pDG was used to produce AAV vector with no detectable adenovirus or wild-type AAV contamination. AAV vector, purified using iodixanol gradient/HI-Q FPLC chromatography, was more than 99% pure, as determined by polyacrylamide silver-stained gel electrophoresis. Further purification information has been described previously [19,20].

Subretinal Injection

Mice were subretinally injected with AAV-mOP500-hRS1 when they were 15 days of age. After anesthesia with ip Ketamine (66.7 mg/kg)/Xylazine (11.7 mg/kg), the right eye of each mouse was dilated with 1% atropine sulfate and 2.5% phenylephrine hydrochloride. After 2.5% hydroxypropyl methylcellulose (Eye Supply USA, Tampa, FL, USA) was applied to the cornea it was punctured carefully with a 30G1/2-gauge needle guided by an operating microscope to avoid lens damage. A blunt 33-gauge needle (Hamilton, Reno, NV, USA) was then inserted through the corneal hole, maneuvered around the lens, displacing it medially, and directed toward the subretinal space of the inferior hemisphere. A total of 1 μl volume of vector with fluorescein tracer (0.1 mg/ml) was used for each injection. An antibiotic (Vetropolycin, Pharmaderm, NY, USA) was applied daily to the cornea for 3 days following the procedure.

Western Blot Analysis

Retinas were dissected from three male RS1-KO mice at 3 months postinjection, pooled into separate groups (injected and uninjected, respectively), and homogenized by sonication in a buffer containing 0.23 M sucrose, 2 mM EDTA, 5 mM Tris–HCl (pH 7.5), 0.1 mM phenylmethylsulfonyl fluoride. The samples were centrifuged at 16,000*g* for 10 min and the supernatants were collected. Protein concentrations were determined using the Coomassie Plus protein assay kit (Pierce, Rockford, IL, USA). After the addition of loading buffer (100 mM Tris–HCl, pH 6.8, 4% SDS, 20% glycerol, 200 mM dithiothreitol, 0.02% bromophenol blue), equal amounts (25 μg) of each sample were resolved by SDS–PAGE (10% Tris–glycine gel) and electrotransferred to a polyvinylidene difluoride membrane (Immobilon P; Millipore, Bedford, MA, USA). The membrane was blocked in 5% horse serum in PBS for 1 h at room temperature and incubated overnight with mouse monoclonal antibody 3R10 specific for RS1 protein [7]. The blot was washed three times in PBS containing 0.05% Tween 20 (PBST) and incubated with an anti-mouse IgG-conjugated alkaline phosphatase secondary antibody for 30 min at room temperature. After being washed again three times in PBST, the blot was developed with a color assay using nitroblue tetrazolium and 5-bromo-4-chloro-3-indolyl phosphate.

Scanning-Laser Ophthalmoscopy

Imaging was performed with a Heidelberg retina angiograph (Heidelberg Engineering GmbH, Dossenheim, Germany), a confocal SLO that provides two laser wavelengths for fundus visualization (argon green, 514 nm, and infrared, 835 nm) and two laser wavelengths for angiography (argon blue, 488 nm (barrier 500 nm) for fluorescence angiography, and infrared, 795 nm (barrier 810 nm) for indocyanine green angiography).

Electroretinographic Analysis

For preliminary time-course experiments, a UTAS-E 200 visual electrodiagnostic system (LKC Technologies, Gaithersburg, MD, USA) was employed. Detailed information on the protocol has been previously described [21]. Briefly, mice were dark-adapted overnight and placed under dim red illumination (>650 nm). Dark-adapted animals were anesthetized and the pupils dilated as above. ERGs from both eyes were recorded simultaneously. Gold contact lens electrodes were placed on the eyes with a drop of 2.5% hydroxypropyl methylcellulose (Eye Supply USA). A reference electrode was placed subcutaneously on the head and a ground electrode was placed in the right hind leg. ERGs were recorded at stimulus intensities of 10^{-4}, 10^{-2}, and 3 cd s/m^2 with 10-, 30-, and 60-s interstimulus intervals (ISIs), respectively, between stimulus flashes. Initial ERG analysis at 1 month postinjection showed scotopic ERG impact only at the highest intensity. Thus, this intensity was used throughout the remaining experiments. Five ERG recordings were averaged for each recording at each stimulus. ERG measurements were made at 1, 2, and 3 months postinjection with statistical comparison between injected and uninjected eyes being done using the Student paired *t* test.

For more detailed analysis at 5 months posttreatment, ERGs were obtained according to previously reported procedures [22] in anesthetized mice. The ERG equipment consisted of a Ganzfeld bowl, a DC amplifier, and a PC-based control and recording unit (Toennies Multiliner Vision, Viasys Healthcare, Hoechberg, Germany). Band-pass filter cut-off frequencies were 0.1 and 3000 Hz. Single-flash recordings were obtained under both dark-adapted (scotopic) and light-adapted (photopic) conditions. Light adaptation before the photopic session was performed with a background illumination of 30 cd/m^2 for 10 min. Single-flash stimulus intensities were increased from 10^{-4} to 25 cd s/m^2, divided into 10 steps of 0.5 and 1 log cd s/m^2. Ten responses were averaged with ISIs of either 5 or 17 s (for 1, 3, 10, and 25 cd s/m^2). Flicker stimuli had an intensity of 3 cd s/m^2 with frequencies of 0.5, 1, 2, 3, 5, 10, 15, and 30 Hz.

Immunofluorescence Labeling of Retinal Sections

Antibodies. Cell-specific antibodies used were monoclonal antibodies RS1-3R10 to human RS1 protein [7], 115A10 (ROB) made against rat olfactory bulb (kindly provided by Shinobu C. Fujita, Mitsubishi Kasei Institute of Life Sciences, Tokyo, Japan.), Per 5H2 to peripherin/rds [23], rabbit polyclonal anti-GFAP (dilution 1:200; Sigma–Aldrich, Munich, Germany), and SYP (SVP38) against synaptophysin purchased from Santa Cruz Biotechnology (Santa Cruz, CA, USA).

Immunolabeling. Retinas from injected and uninjected eyes of *Rs1h*-deficient mice 5 month posttreatment and age-matched wild-type C57BL/6 mice were used for immunocytochemical labeling studies.

Whole eyes were fixed with 4% paraformaldehyde in 0.1 M phosphate buffer (pH 7.4) for 4 h and subsequently rinsed in 0.1 M phosphate buffer containing 10% sucrose. Cryosections were permeabilized and blocked with PBS containing 0.2% Triton X-100 and 10% normal goat serum for 20 min and labeled overnight with the primary antibody diluted in PBS containing 0.1% Triton X-100 and 2.5% normal goat serum. Sections were rinsed in PBS containing 0.01% Tween 20 and labeled for 1 h with Alexa 488-conjugated goat anti-mouse immunoglobulin (Molecular Probes, Eugene, OR, USA). Labeled sections were also stained with DAPI nuclear stain and examined under a Zeiss LSM510 confocal microscope and processed with Zeiss LSM5 Image Browser. Counting of labeled cells was carried out on a Zeiss Axioplan 2 fluorescence microscope equipped with Northern Eclipse digital image analysis system.

ACKNOWLEDGMENTS

This work was supported by NIH EY11123 (W.W.H.), EY02422 (R.M.), and NS36302 (W.W.H.); the Macula Vision Research Foundation (B.H.F.W., R.M., W.W.H.); the Foundation Fighting Blindness (B.H.F.W., R.M., W.W.H.); Research to Prevent Blindness, Inc. (W.W.H.); German Research Council DFG Se837/4-1 (M.W.S.), University of Tübingen 1173-0-0 (M.W.S.); and European Community Grant EVI-Genoret (M.W.S.). W.W.H. and the University of Florida own equity in a company, Applied Genetic Technologies Corp., that may commercialize some of the technology described in this work.

RECEIVED FOR PUBLICATION APRIL 16, 2005; REVISED JUNE 3, 2005; ACCEPTED JUNE 6, 2005.

REFERENCES

1. Mooy, C. M., *et al.* (2002). Hereditary X-linked juvenile retinoschisis: a review of the role of Muller cells. *Arch. Ophthalmol.* **120:** 979–984.
2. Sauer, C. G., *et al.* (1997). Positional cloning of the gene associated with X-linked juvenile retinoschisis. *Nat. Genet.* **17:** 164–170.
3. Molday, L. L., Hicks, D., Sauer, C. G., Weber, B. H., and Molday, R. S. (2001). Expression of X-linked retinoschisis protein RS1 in photoreceptor and bipolar cells. *Invest. Ophthalmol. Visual Sci.* **42:** 816–825.
4. Reid, S. N., Yamashita, C., and Farber, D. B. (2003). Retinoschisin, a photoreceptor-secreted protein, and its interaction with bipolar and Muller cells. *J. Neurosci.* **23:** 6030–6040.
5. Wu, W. W., and Molday, R. S. (2003). Defective discoidin domain structure, subunit assembly, and endoplasmic reticulum processing of retinoschisin are primary mechanisms responsible for X-linked retinoschisis. *J. Biol. Chem.* **278:** 28139–28146.
6. Wang, T., *et al.* (2002). Intracellular retention of mutant retinoschisin is the pathological mechanism underlying X-linked retinoschisis. *Hum. Mol. Genet.* **11:** 3097–3105.
7. Weber, B. H., *et al.* (2002). Inactivation of the murine X-linked juvenile retinoschisis gene, Rs1h, suggests a role of retinoschisin in retinal cell layer organization and synaptic structure. *Proc. Natl. Acad. Sci. USA* **99:** 6222–6227.
8. Gehrig, A. E., Warneke-Wittstock, R., Sauer, C. G., and Weber, B. H. (1999). Isolation and characterization of the murine X-linked juvenile retinoschisis (Rs1h) gene. *Mamm. Genome* **10:** 303–307.
9. Seeliger, M. W., *et al.* (2003). MfERG waveform characteristics in the RS1h mouse model featuring a 'negative' ERG. *Doc. Ophthalmol.* **107:** 37–44.
10. Zeng, Y., *et al.* (2004). RS-1 gene delivery to an adult Rs1h knockout mouse model restores ERG b-wave with reversal of the electronegative waveform of X-linked retinoschisis. *Invest. Ophthalmol. Visual Sci.* **45:** 3279–3285.
11. Lewis, G. P., Erickson, P. A., Guerin, C. J., Anderson, D. H., and Fisher, S. K. (1992). Basic fibroblast growth factor: a potential regulator of proliferation and intermediate filament expression in the retina. *J. Neurosci.* **12:** 3968–3978.
12. Bravo-Nuevo, A., Walsh, N., and Stone, J. (2004). Photoreceptor degeneration and loss of retinal function in the C57BL/6-C2J mouse. *Invest. Ophthalmol. Visual Sci.* **45:** 2005–2012.
13. Smith, S. B., Brodjian, S., Desai, S., and Sarthy, V. (1997). Glial fibrillary acidic protein (GFAP) is synthesized in the early stages of the photoreceptor cell degeneration of the mivit/mivit (vitiligo) mouse. *Exp. Eye Res.* **64:** 645–650.
14. Rabinowitz, J. E., *et al.* (2002). Cross-packaging of a single adeno-associated virus (AAV) type 2 vector genome into multiple AAV serotypes enables transduction with broad specificity. *J. Virol.* **76:** 791–801.
15. Yang, G. S., *et al.* (2002). Virus-mediated transduction of murine retina with adeno-associated virus: effects of viral capsid and genome size. *J. Virol.* **76:** 7651–7660.
16. Flannery, J. G., *et al.* (1997). Efficient photoreceptor-targeted gene expression in vivo by recombinant adeno-associated virus. *Proc. Natl. Acad. Sci. USA* **94:** 6916–6921.
17. Auricchio, A., *et al.* (2001). Exchange of surface proteins impacts on viral vector cellular specificity and transduction characteristics: the retina as a model. *Hum. Mol. Genet.* **10:** 3075–3081.
18. Martin, K. R., *et al.* (2003). Gene therapy with brain-derived neurotrophic factor as a protection: retinal ganglion cells in a rat glaucoma model. *Invest. Ophthalmol. Visual Sci.* **44:** 4357–4365.
19. Zolotukhin, S., Potter, M., Hauswirth, W. W., Guy, J., and Muzyczka, N. (1996). A "humanized" green fluorescent protein cDNA adapted for high-level expression in mammalian cells. *J. Virol.* **70:** 4646–4654.
20. Zolotukhin, S., *et al.* (1999). Recombinant adeno-associated virus purification using novel methods improves infectious titer and yield. *Gene Ther.* **6:** 973–985.
21. Timmers, A. M., Zhang, H., Squitieri, A., and Gonzalez-Pola, C. (2001). Subretinal injections in rodent eyes: effects on electrophysiology and histology of rat retina. *Mol. Vision* **7:** 131–137.
22. Seeliger, M. W., *et al.* (2001). New views on RPE65 deficiency: the rod system is the source of vision in a mouse model of Leber congenital amaurosis. *Nat. Genet.* **29:** 70–74.
23. Connell, G., *et al.* (1991). Photoreceptor peripherin is the normal product of the gene responsible for retinal degeneration in the rds mouse. *Proc. Natl. Acad. Sci. USA* **88:** 723–726.